

Topology of Monitored Quantum Dynamics

Zhenyu Xiao^{1,*} and Kohei Kawabata^{2,†}

¹*International Center for Quantum Materials, Peking University, Beijing 100871, China*

²*Institute for Solid State Physics, University of Tokyo, Kashiwa, Chiba 277-8581, Japan*

(Dated: December 10, 2024)

The interplay between unitary dynamics and quantum measurements induces a variety of open quantum phenomena that have no counterparts in closed quantum systems at equilibrium. Here, we generally classify Kraus operators and their effective non-Hermitian dynamical generators within the 38-fold way, thereby establishing the tenfold classification for symmetry and topology of monitored free fermions. Our classification elucidates the role of topology in measurement-induced phase transitions and identifies potential topological terms in the corresponding nonlinear sigma models. Furthermore, we demonstrate that nontrivial topology in spacetime manifests itself as anomalous boundary states in Lyapunov spectra, such as Lyapunov zero modes and chiral edge modes, constituting the bulk-boundary correspondence in monitored quantum dynamics.

The interplay of unitary dynamics and quantum measurements gives rise to distinctive phenomena in open quantum systems with no analogs in closed quantum systems at equilibrium [1]. Generally, open quantum dynamics is not described by Hermitian Hamiltonians but by nonunitary Kraus operators [2–4], in which measurements select a quantum trajectory [5–7]. Unitary dynamics accompanies the propagation of quantum correlations and entanglement, resulting in thermalization [8–10]. By contrast, nonunitary quantum measurements drive the system into nonequilibrium steady states. Their competition has been shown to induce dynamical quantum phase transitions [11–18], extensively investigated in both theory [19–48] and experiments [49–51].

Monitored free fermions exhibit rich open quantum phenomena and have attracted considerable recent interest [52–77]. Numerical investigations found measurement-induced phase transitions for monitored complex [73, 74] and Majorana [53, 65] fermions in two and one spatial dimensions, respectively, despite their possible absence for complex fermions in one dimension [52, 55]. Symmetry of nonunitary quantum circuits was also studied through a tensor-network framework [39]. While this analysis corresponds to forced measurements with postselected quantum trajectories, subsequent works developed effective nonlinear sigma model descriptions for monitored free fermions [68, 70, 72], reminiscent of those for the Anderson transitions in disordered electron systems [78–82]. Accordingly, the unique finite-size scaling of entanglement entropy was perturbatively derived, consistent with numerical calculations.

Still, the intricate connection between these effective field theory and microscopic nonunitary quantum dynamics has not been fully understood. Specifically, topological terms can generally be incorporated into nonlinear sigma models, which profoundly influence the Anderson transitions, as exemplified by the quantum Hall transitions [83–85]. They also underlie the celebrated tenfold classification of topological insulators and superconductors [86–91]. However, the role of topology in monitored

quantum dynamics has remained largely elusive.

In this Letter, we establish the classification of symmetry and topology for monitored free fermions. While generic non-Hermitian operators are categorized into the 38-fold symmetry classification [92, 93], we identify the relevant tenfold symmetry classes for single-particle Kraus operators and associated non-Hermitian dynamical generators (Table I). Building upon this symmetry classification, we comprehensively classify topology of single-particle monitored quantum dynamics (Table II). This classification reveals the role of topology in measurement-induced phase transitions and describes potential topological terms in the underlying nonlinear sigma models. Moreover, we demonstrate that nontrivial non-Hermitian topology in spacetime gives rise to anomalous boundary states in Lyapunov spectra, thereby serving as the bulk-boundary correspondence in monitored quantum dynamics.

Monitored quantum dynamics.—We study the general nonunitary quantum dynamics of monitored free fermions in d spatial dimensions. Owing to the free-fermion nature, the dynamics preserves Gaussianity and is fully encoded in single-particle Kraus operators [77, 95]. We divide time into infinitesimal intervals Δt and consider the Kraus operator K_t at each time step that incorporates both random unitary evolution and stochastic nonunitary measurements. The cumulative Kraus operator $K_{[0,t]}$ over the time interval $[0, t]$ is

$$K_{[0,t]} := K_t K_{t-\Delta t} \cdots K_{\Delta t}, \quad (1)$$

which specifies a single-particle quantum trajectory [96, 97]. Over an infinitesimal interval $[t, t+\Delta t]$, a wave function $|\psi_t\rangle$ evolves as $|\psi_{t+\Delta t}\rangle \propto K_t |\psi_t\rangle$. By the expansion $K_t =: e^{H_t \Delta t}$, the time evolution is also described by the stochastic Schrödinger equation,

$$L_t |\psi_t\rangle = 0, \quad L_t := \partial_t - H_t, \quad (2)$$

where L_t serves as an effective non-Hermitian operator governing the nonunitary quantum dynamics. Notably,

TABLE I. Tenfold symmetry classification of single-particle Kraus operators K and the associated non-Hermitian dynamical generators L based on time-reversal symmetry (TRS), particle-hole symmetry (PHS), and chiral symmetry (CS). The classifying spaces of K correspond to noncompact types (see, for example, Table I in Ref. [94] and Table IV in Ref. [82]). The column ‘‘Classifying space (L)’’ also shows the symmetry classes of the corresponding Hermitian Hamiltonians with the same classifying spaces in the brackets.

Class	TRS \mathcal{T}	PHS \mathcal{C}	CS Γ	Classifying space (K)	Classifying space (L)
A	0	0	0	$\text{GL}(N, \mathbb{C})/\text{U}(N) \cong \mathcal{C}_1$	\mathcal{C}_1 (AIII)
AIII	0	0	1	$\text{U}(N, N)/\text{U}(N) \times \text{U}(N) \cong \mathcal{C}_0$	\mathcal{C}_0 (A)
AI	+1	0	0	$\text{GL}(N, \mathbb{R})/\text{O}(N) \cong \mathcal{R}_7$	\mathcal{R}_1 (BDI)
BDI	+1	+1	1	$\text{O}(N, N)/\text{O}(N) \times \text{O}(N) \cong \mathcal{R}_0$	\mathcal{R}_2 (D)
D	0	+1	0	$\text{O}(N, \mathbb{C})/\text{O}(N) \cong \mathcal{R}_1$	\mathcal{R}_3 (DIII)
DIII	-1	+1	1	$\text{O}^*(2N)/\text{U}(N) \cong \mathcal{R}_2$	\mathcal{R}_4 (AII)
AII	-1	0	0	$\text{U}^*(2N)/\text{Sp}(N) \cong \mathcal{R}_3$	\mathcal{R}_5 (CII)
CII	-1	-1	1	$\text{Sp}(N, N)/\text{Sp}(N) \times \text{Sp}(N) \cong \mathcal{R}_4$	\mathcal{R}_6 (C)
C	0	-1	0	$\text{Sp}(N, \mathbb{C})/\text{Sp}(N) \cong \mathcal{R}_5$	\mathcal{R}_7 (CI)
CI	+1	-1	1	$\text{Sp}(N, \mathbb{R})/\text{U}(N) \cong \mathcal{R}_6$	\mathcal{R}_0 (AI)

TABLE II. Tenfold topological classification of single-particle monitored quantum dynamics L in d spatial dimensions and one temporal dimension. The classification reduces to the point-gap topology in the Altland-Zirnbauer symmetry class [93].

Class		$d+1=1$	$d+1=2$	$d+1=3$	$d+1=4$	$d+1=5$	$d+1=6$	$d+1=7$	$d+1=8$
A	\mathcal{C}_1	\mathbb{Z}	0	\mathbb{Z}	0	\mathbb{Z}	0	\mathbb{Z}	0
AIII	\mathcal{C}_0	0	\mathbb{Z}	0	\mathbb{Z}	0	\mathbb{Z}	0	\mathbb{Z}
AI	\mathcal{R}_1	\mathbb{Z}	0	0	0	$2\mathbb{Z}$	0	\mathbb{Z}_2	\mathbb{Z}_2
BDI	\mathcal{R}_2	\mathbb{Z}_2	\mathbb{Z}	0	0	0	$2\mathbb{Z}$	0	\mathbb{Z}_2
D	\mathcal{R}_3	\mathbb{Z}_2	\mathbb{Z}_2	\mathbb{Z}	0	0	0	$2\mathbb{Z}$	0
DIII	\mathcal{R}_4	0	\mathbb{Z}_2	\mathbb{Z}_2	\mathbb{Z}	0	0	0	$2\mathbb{Z}$
AII	\mathcal{R}_5	$2\mathbb{Z}$	0	\mathbb{Z}_2	\mathbb{Z}_2	\mathbb{Z}	0	0	0
CII	\mathcal{R}_6	0	$2\mathbb{Z}$	0	\mathbb{Z}_2	\mathbb{Z}_2	\mathbb{Z}	0	0
C	\mathcal{R}_7	0	0	$2\mathbb{Z}$	0	\mathbb{Z}_2	\mathbb{Z}_2	\mathbb{Z}	0
CI	\mathcal{R}_0	0	0	0	$2\mathbb{Z}$	0	\mathbb{Z}_2	\mathbb{Z}_2	\mathbb{Z}

the relationship between L_t and K_t is analogous to that between Hamiltonians and their transfer matrices in disordered electron systems [81, 82], where the temporal direction is replaced with the spatial direction.

Symmetry.—Both K_t and L_t are categorized into the 38-fold classification of non-Hermitian operators [92, 93]. Importantly, they inherently incorporate spacetime randomness arising from both spatial disorder and temporal noise intrinsic to quantum measurements. Consequently, only symmetries preserved by the product of Kraus operators in Eq. (1) at each spacetime are relevant to the physics of monitored free fermions, including their topological phenomena and measurement-induced phase transitions. We identify such spacetime internal symmetries as

$$\mathcal{T}K_t^*\mathcal{T}^{-1} = K_t \quad (\mathcal{T}\mathcal{T}^* = \pm 1), \quad (3)$$

$$\mathcal{C}(K_t^T)^{-1}\mathcal{C}^{-1} = K_t \quad (\mathcal{C}\mathcal{C}^* = \pm 1), \quad (4)$$

$$\Gamma(K_t^\dagger)^{-1}\Gamma^{-1} = K_t \quad (\Gamma^2 = 1), \quad (5)$$

with unitary operators \mathcal{T} , \mathcal{C} , and Γ . Transposition and inversion reverse the temporal direction and therefore do not appear alone in quantum trajectories. Even if each Kraus operator satisfies $K_t^T = K_t$ ($K_t^{-1} = K_t$), their product generally satisfies $(K_s K_t)^T = K_t^T K_s^T \neq K_s^T K_t^T$

$[(K_s K_t)^{-1} = K_t^{-1} K_s^{-1} \neq K_s^{-1} K_t^{-1}]$. However, their combined action can be respected as in Eqs. (4) and (5). Accordingly, the non-Hermitian dynamical generator L respects

$$\mathcal{T}L_t^*\mathcal{T}^{-1} = L_t \quad (\mathcal{T}\mathcal{T}^* = \pm 1), \quad (6)$$

$$\mathcal{C}L_t^T\mathcal{C}^{-1} = -L_t \quad (\mathcal{C}\mathcal{C}^* = \pm 1), \quad (7)$$

$$\Gamma L_t^\dagger \Gamma^{-1} = -L_t \quad (\Gamma^2 = 1). \quad (8)$$

Within the 38-fold classification [93], these symmetries are called time-reversal, particle-hole, and chiral symmetries, respectively, constituting the tenfold classification (Table I).

Depending on symmetry, K_t and L_t belong to different classifying spaces. Owing to non-Hermiticity, these classifying spaces correspond to noncompact types [94, 99]. While our symmetry classification is consistent with the tensor-network framework [56], it extends its applicability to encompass more generic nonunitary quantum dynamics, including those arising from Born measurements. Although Eqs. (3) and (6) are referred to as time-reversal symmetry for notational convenience, they do not correspond to the physical time-reversal operation. Indeed, physical time-reversal symmetry, $\mathcal{T}K_t^*\mathcal{T}^{-1} = K_{-t}$, no longer serves as internal symmetry in spacetime, and

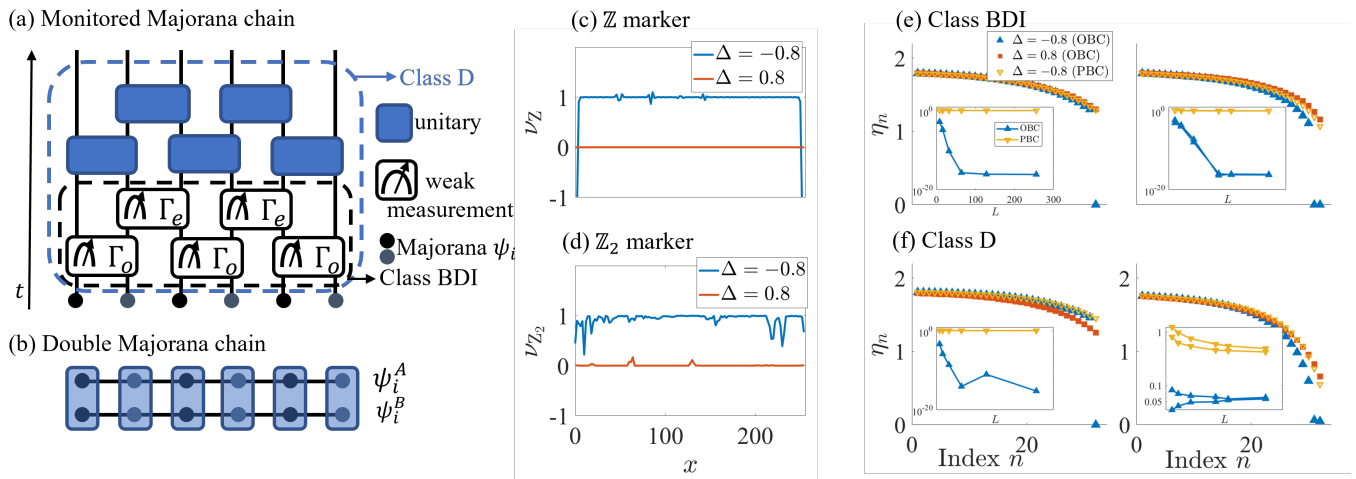


FIG. 1. (a) Monitored dynamics of a Majorana chain generated by repeating the operations inside the black (blue) dashed lines for class BDI (D). (b) Monitored dynamics of the double Majorana chain generated by the operations in subfigure (a) on individual chains and the unitary gates coupling the two chains. (c) \mathbb{Z} and (d) \mathbb{Z}_2 topological markers for the steady states in classes BDI and D, respectively. The fluctuations are due to the spatial randomness in $K_{[0,t]}$. (e), (f) Lyapunov spectra of the monitored single (left) and double (right) Majorana chains in classes (e) BDI and (f) D. Insets: smallest (or two smallest) positive Lyapunov exponent(s) as a function of the system size. Due to particle-hole symmetry, Lyapunov exponents appear in opposite-sign pairs $(\eta_i, -\eta_i)$, and only $\eta_i \geq 0$ is shown. Details of the models can be found in Ref. [98].

is thus irrelevant to the monitored quantum dynamics. Moreover, chiral symmetry in Eqs. (5) and (8) is equivalent to (pseudo-)unitarity of transfer matrices [81].

Topology.—To characterize the non-Hermitian dynamical generator L_t from the topological perspective, we introduce a Hermitized operator [93, 100]

$$\tilde{L}_t := \begin{pmatrix} 0 & L_t \\ L_t^\dagger & 0 \end{pmatrix}. \quad (9)$$

Non-Hermitian topology of L_t is equivalent to Hermitian topology of \tilde{L}_t . By construction, \tilde{L}_t respects additional chiral symmetry, $\sigma_z \tilde{L}_t \sigma_z^{-1} = -\tilde{L}_t$ with a Pauli matrix σ_z , changing the relevant symmetry classes, as also listed in Table I. We thus develop the tenfold topological classification of non-Hermitian dynamical generators L_t in $(d+1)$ -dimensional spacetime in Table II. It applies to both Born and forced measurements since the classifying spaces are common. From the homotopy perspective, topology is captured by $\pi_0(\mathcal{C}_{s-(d+1)})$ or $\pi_0(\mathcal{R}_{s-(d+1)})$.

Analogous to topological insulators and superconductors at equilibrium [86–91], Table II hosts twofold or eightfold periodicity with respect to spacetime dimensions $d+1$. This directly arises from the Bott periodicity in K -theory [101]. We stress that Table II differs from the classification of Kraus operators K_t or Lindbladians, which reduces to a different tenfold way [102–106]. We also derive such alternative tenfold topological classification of K_t [98]. By contrast, the tenfold way in Table II describes possible topological terms in the effective nonlinear sigma models [68, 70, 72], elucidating topological measurement-induced phase transitions. In zero spatial

dimension $d=0$, topology can protect dynamical quantum criticality with divergent purification time [77], akin to disordered chiral-symmetric [107–110] and nonreciprocal [111, 112] wires [98].

Bulk-boundary correspondence.—We further demonstrate that spacetime topology of L_t induces topology of steady states and concomitant anomalous boundary states in Lyapunov spectra. The purification time quantifying the decay of entropy is given as $\tau_P = 2/\min_n |\eta_n|$, where the Lyapunov exponents η_n 's are defined through singular values $e^{\lambda_n(t)}$'s of $K_{[0,t]}$ as $\eta_n := \lim_{t \rightarrow \infty} \lambda_n(t)/t$. According to the Oseledets theorem [113], we also have $\eta_n = \text{Re } z_n$ for $t \rightarrow \infty$, where z_n 's are complex eigenvalues of a non-Hermitian operator \bar{H}_t defined by $K_{[0,t]} := e^{\bar{H}_t t}$. If $\text{Re } z_i$'s exhibit a gap with respect to $\text{Re } z = 0$ (i.e., real line gap [93]), τ_P is finite; otherwise, it diverges. As discussed above, non-Hermiticity of L_t changes the relevant classifying spaces. Meanwhile, unlike the equilibrium counterparts in d spatial dimensions, L_t operates in $(d+1)$ -dimensional spacetime. These combined changes lead to the coincidence of Table II with the periodic table at equilibrium. Consequently, the topological classification of L_t generally coincides with that of gapped \bar{H}_t with finite τ_P . In the topological phase, while \bar{H}_t is gapped under the periodic boundary conditions (PBC), it becomes gapless under the open boundary conditions (OBC) due to the emergence of anomalous boundary states, resulting in the topologically protected divergence of τ_P .

Moreover, topology of \bar{H}_t manifests itself in the steady-state correlation function $C_{ij} := \langle \Psi_S | c_i^\dagger c_j | \Psi_S \rangle -$

$\delta_{ij}/2$ with fermionic annihilation (creation) operators c_i 's (c_i^\dagger 's). For a generic initial density matrix, the steady state $|\Psi_S\rangle$ is the many-body eigenstate with the largest norm of the eigenvalue, obtained as $|\Psi_S\rangle \propto \prod_{n=1}^p \left(\sum_i c_i^\dagger (\vec{R}_n)_i \right) |0\rangle$, where \vec{R}_n 's are right eigenvectors of \bar{H}_t with the eigenvalues $\text{Re } z_n > 0$ ($i = 1, \dots, p$), and $|0\rangle$ is the fermionic vacuum state. Thus, \bar{H}_t is continuously deformable into C while preserving the real line gap and symmetry. To obtain the topological invariant of L_t or \bar{H}_t , it suffices to evaluate that of C using tools developed for disordered topological insulators.

Lyapunov zero modes in 1+1 dimensions.—As an illustrative example, we consider circuit models of measurement-only dynamics of Majorana chains, generated by iterative weak Born measurements on neighboring Majorana pairs [Fig. 1 (a)]. The odd pairs $i\psi_{2i-1}\psi_{2i}$ ($i = 1, 2, \dots, L/2$) are measured with strength $\Gamma_o = \Gamma(1 + \Delta)$, while the even pairs $i\psi_{2i}\psi_{2i+1}$ with $\Gamma_e = \Gamma(1 - \Delta)$. Besides particle-hole symmetry in Eq. (7) inherent in Majorana fermions, L_t and \bar{H}_t respect additional chiral symmetry in Eq. (8) and hence belong to class BDI. They exhibit \mathbb{Z} -classified topology (see Table II), characterized by the winding number for \bar{H}_t and the Chern number for L_t . For $\Delta < 0$, the stronger measurements on the even pairs $i\psi_{2i}\psi_{2i+1}$ enhance pairing between them, leaving the Majoranas at the edges unpaired under OBC, reminiscent of topological superconducting wires [114]. Numerically simulating the dynamics and calculating the local chiral index $\nu_Z \in \mathbb{Z}$ of \bar{H}_t [98, 109, 115], we confirm $\nu_Z = 1$ ($\nu_Z = 0$) for $\Delta < 0$ ($\Delta > 0$) [Fig. 1(c)]. While the Lyapunov spectra exhibit a gap in both topological and trivial phases under PBC (i.e., $\min_n |\eta_n| > 0$), the topological phase features a zero mode under OBC [Fig. 1(d)], representing the bulk-boundary correspondence and stabilizing algebraically slow purification dynamics.

When generic unitary operations are introduced, the symmetry class is reduced to class D, governed by the \mathbb{Z}_2 topology. We find that weak unitary operations do not close the gap, leading to $\nu_{\mathbb{Z}_2} = 1$ ($\nu_{\mathbb{Z}_2} = 0$) for $\Delta < 0$ ($\Delta > 0$) [Fig. 1(d)]. In the topological phase $\nu_{\mathbb{Z}_2} = 1$, a zero mode persists in the Lyapunov spectra under OBC [Fig. 1(f)]. The distinction between the \mathbb{Z} and \mathbb{Z}_2 topology manifests itself by coupling two topologically nontrivial Majorana chains [Fig. 1(b)]. We add a symmetry-preserving unitary gate $e^{\phi_i \psi_i^A \psi_i^B}$ ($\phi_i \in \mathbb{R}$), with A and B being the chain indices. While two Lyapunov zero modes survive in class BDI, they can be lifted in class D, consistent with the \mathbb{Z}_2 classification [Fig. 1(e), (f)].

In the measurement-only dynamics (class BDI), the perturbative expansion of the beta function for the corresponding nonlinear sigma model reads, $\beta(t) = d - 1 - 4t^3 + \mathcal{O}(t^4)$, with the coupling parameter $t \geq 0$ [82, 116–118]. Notably, we always have $\beta < 0$ for $d \leq 1$, preclud-

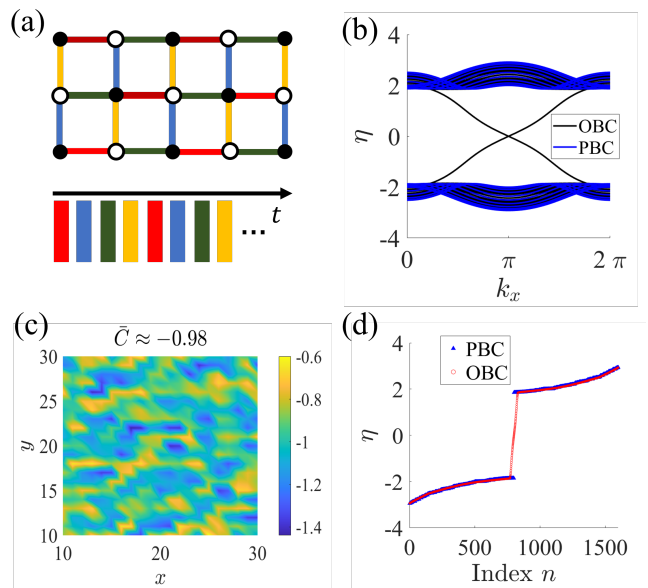


FIG. 2. (a) $(2+1)$ -dimensional quantum circuit on a lattice of size $L_x \times L_y$. Each site \mathbf{r} incorporates one fermion c_r^\dagger . At each time step, measurements and unitary gates are applied to the bonds of a specific color, following the sequence shown at the bottom. (b) Lyapunov spectra of the dynamics with the homogeneous measurement strength under the periodic boundary conditions (PBC) along the x direction, and PBC or open boundary conditions (OBC) along the y direction. (c), (d) Monitored dynamics with inhomogeneous measurement strength: (c) Local Chern marker of the steady state. (d) Lyapunov spectra under PBC and OBC. Details of the models can be found in Ref. [98].

ing measurement-induced phase transitions. Nevertheless, numerical simulations of lattice models support their presence [53, 65, 70, 119]. This implies that the phase transitions therein cannot be explained by the standard nonlinear sigma model but that with a topological term. Consistently, the \mathbb{Z} -classified topology in Table II corresponds to a θ term, inducing critical behavior even for $d = 1$, akin to the quantum Hall transitions [83–85]. This also shows the significance of topology in measurement-induced phase transitions.

Lyapunov chiral edge modes in 2+1 dimensions.—We further investigate monitored complex fermions on a square lattice where unitary gates [120] and weak measurements are applied to the bonds of neighboring sites, with postselections on measurement outcomes [Fig. 2(a)]. The dynamics belongs to class A, characterized by the Chern number for \bar{H}_t and the $(2+1)$ -dimensional winding number for L_t . We first consider a scenario where the measurement strengths are uniform across all bonds and constant over time, preserving translation invariance both temporally and spatially. We find that the local Chern marker is quantized as $C(\mathbf{r}) \approx -1$ in the steady state [98, 115, 121]. This nontrivial Chern number also accompanies gapless modes in Lyapunov

spectra under OBC [Fig. 2(b)], analogous to chiral edge modes in the quantum Hall effect. We also consider another scenario where measurement strengths vary randomly among bonds and time, thereby breaking translational invariance. While the local Chern marker $C(\mathbf{r})$ becomes spatially inhomogeneous, its average $\bar{C}(\mathbf{r})$ over the central range of the lattice remains close to -1 [Fig. 2(c)]. The Lyapunov spectra retain the gapless modes under OBC [Fig. 2(d)].

Discussions.—In this Letter, we establish the tenfold classification of symmetry and topology for monitored free fermions. Based on this classification, we elucidate topological phase transitions and bulk-boundary correspondence in monitored quantum dynamics. Our classification represents an open quantum analog of the periodic table of topological insulators and superconductors [86–91], and provides a guiding principle to investigate monitored free fermions across various symmetry classes and spacetime dimensions. For example, a recent work [122] has found a unique entanglement structure due to the presence of a domain wall. It merits further study to explore its possible connection with our framework. Moreover, it should be significant to incorporate many-body interactions into our framework, akin to equilibrium counterparts. Finally, it is worth noting that non-Hermitian topology causes anomalous boundary phenomena including the skin effect [123–128], which should also be relevant to the universality classes of measurement-induced phase transitions [63, 64, 75, 129].

Note added.—After the completion of this work, we became aware of a recent related work [130].

Acknowledgment.—We thank Tomi Ohtsuki, Shinsei Ryu, and Ryuichi Shindou for helpful discussion. We thank Ryusuke Hamazaki for coordinating the submission of this work and Ref. [130]. Z.X. is supported by the National Basic Research Programs of China (No. 2019YFA0308401) and by the National Natural Science Foundation of China (No. 11674011 and No. 12074008). K.K. is supported by MEXT KAKENHI Grant-in-Aid for Transformative Research Areas A “Extreme Universe” No. 24H00945.

* wjxzy@pku.edu.cn

† kawabata@issp.u-tokyo.ac.jp

- [1] M. P. Fisher, V. Khemani, A. Nahum, and S. Vijay, *Random Quantum Circuits*, *Annu. Rev. Condens. Matter Phys.* **14**, 335 (2023).
- [2] M. A. Nielsen and I. L. Chuang, *Quantum Computation and Quantum Information* (Cambridge University Press, Cambridge, England, 2000).
- [3] H.-P. Breuer and F. Petruccione, *The Theory of Open Quantum Systems* (Oxford University Press, Oxford, 2007).

- [4] A. Rivas and S. F. Huelga, *Open Quantum Systems* (Springer, Berlin, Heidelberg, 2012).
- [5] H. Carmichael, *An Open Systems Approach to Quantum Optics* (Springer, Berlin, 1993).
- [6] M. B. Plenio and P. L. Knight, The quantum-jump approach to dissipative dynamics in quantum optics, *Rev. Mod. Phys.* **70**, 101 (1998).
- [7] A. J. Daley, Quantum trajectories and open many-body quantum systems, *Adv. Phys.* **63**, 77 (2014).
- [8] J. Eisert, M. Friesdorf, and C. Gogolin, Quantum many-body systems out of equilibrium, *Nat. Phys.* **11**, 124 (2015).
- [9] R. Nandkishore and D. A. Huse, Many-Body Localization and Thermalization in Quantum Statistical Mechanics, *Annu. Rev. Condens. Matter Phys.* **6**, 15 (2015).
- [10] L. D’Alessio, Y. Kafri, A. Polkovnikov, and M. Rigol, From quantum chaos and eigenstate thermalization to statistical mechanics and thermodynamics, *Adv. Phys.* **65**, 239 (2016).
- [11] R. Vasseur, A. C. Potter, Y.-Z. You, and A. W. W. Ludwig, Entanglement transitions from holographic random tensor networks, *Phys. Rev. B* **100**, 134203 (2019).
- [12] A. Chan, R. M. Nandkishore, M. Pretko, and G. Smith, Unitary-projective entanglement dynamics, *Phys. Rev. B* **99**, 224307 (2019).
- [13] B. Skinner, J. Ruhman, and A. Nahum, Measurement-Induced Phase Transitions in the Dynamics of Entanglement, *Phys. Rev. X* **9**, 031009 (2019).
- [14] Y. Li, X. Chen, and M. P. A. Fisher, Quantum Zeno effect and the many-body entanglement transition, *Phys. Rev. B* **98**, 205136 (2018).
- [15] Y. Li, X. Chen, and M. P. A. Fisher, Measurement-driven entanglement transition in hybrid quantum circuits, *Phys. Rev. B* **100**, 134306 (2019).
- [16] S. Choi, Y. Bao, X.-L. Qi, and E. Altman, Quantum Error Correction in Scrambling Dynamics and Measurement-Induced Phase Transition, *Phys. Rev. Lett.* **125**, 030505 (2020).
- [17] M. J. Gullans and D. A. Huse, Dynamical Purification Phase Transition Induced by Quantum Measurements, *Phys. Rev. X* **10**, 041020 (2020).
- [18] C.-M. Jian, Y.-Z. You, R. Vasseur, and A. W. W. Ludwig, Measurement-induced criticality in random quantum circuits, *Phys. Rev. B* **101**, 104302 (2020).
- [19] M. Szyniszewski, A. Romito, and H. Schomerus, Entanglement transition from variable-strength weak measurements, *Phys. Rev. B* **100**, 064204 (2019).
- [20] Y. Bao, S. Choi, and E. Altman, Theory of the phase transition in random unitary circuits with measurements, *Phys. Rev. B* **101**, 104301 (2020).
- [21] Q. Tang and W. Zhu, Measurement-induced phase transition: A case study in the nonintegrable model by density-matrix renormalization group calculations, *Phys. Rev. Research* **2**, 013022 (2020).
- [22] M. J. Gullans and D. A. Huse, Scalable Probes of Measurement-Induced Criticality, *Phys. Rev. Lett.* **125**, 070606 (2020).
- [23] A. Zabalo, M. J. Gullans, J. H. Wilson, S. Gopalakrishnan, D. A. Huse, and J. H. Pixley, Critical properties of the measurement-induced transition in random quantum circuits, *Phys. Rev. B* **101**, 060301 (2020).
- [24] S. Goto and I. Danshita, Measurement-induced transitions of the entanglement scaling law in ultracold gases

- with controllable dissipation, *Phys. Rev. A* **102**, 033316 (2020).
- [25] A. Lavasani, Y. Alavirad, and M. Barkeshli, Measurement-induced topological entanglement transitions in symmetric random quantum circuits, *Nat. Phys.* **17**, 342 (2021).
- [26] S. Sang and T. H. Hsieh, Measurement-protected quantum phases, *Phys. Rev. Research* **3**, 023200 (2021).
- [27] M. Ippoliti, M. J. Gullans, S. Gopalakrishnan, D. A. Huse, and V. Khemani, Entanglement Phase Transitions in Measurement-Only Dynamics, *Phys. Rev. X* **11**, 011030 (2021).
- [28] M. Sznyszewski, A. Romito, and H. Schomerus, Universality of Entanglement Transitions from Stroboscopic to Continuous Measurements, *Phys. Rev. Lett.* **125**, 210602 (2020).
- [29] O. Lunt and A. Pal, Measurement-induced entanglement transitions in many-body localized systems, *Phys. Rev. Research* **2**, 043072 (2020).
- [30] Y. Li and M. P. A. Fisher, Statistical mechanics of quantum error correcting codes, *Phys. Rev. B* **103**, 104306 (2021).
- [31] L. Fidkowski, J. Haah, and M. B. Hastings, How Dynamical Quantum Memories Forget, *Quantum* **5**, 382 (2021).
- [32] A. Nahum, S. Roy, B. Skinner, and J. Ruhman, Measurement and Entanglement Phase Transitions in All-To-All Quantum Circuits, on Quantum Trees, and in Landau-Ginsburg Theory, *PRX Quantum* **2**, 010352 (2021).
- [33] M. Ippoliti and V. Khemani, Postselection-Free Entanglement Dynamics via Spacetime Duality, *Phys. Rev. Lett.* **126**, 060501 (2021).
- [34] A. Biella and M. Schirò, Many-Body Quantum Zeno Effect and Measurement-Induced Subradiance Transition, *Quantum* **5**, 528 (2021).
- [35] Y. Bao, S. Choi, and E. Altman, Symmetry enriched phases of quantum circuits, *Ann. Phys.* **435**, 168618 (2021).
- [36] T.-C. Lu and T. Grover, Spacetime duality between localization transitions and measurement-induced transitions, *PRX Quantum* **2**, 040319 (2021).
- [37] M. Ippoliti, T. Rakovszky, and V. Khemani, Fractal, Logarithmic, and Volume-Law Entangled Nonthermal Steady States via Spacetime Duality, *Phys. Rev. X* **12**, 011045 (2022).
- [38] X. Turkeshi, A. Biella, R. Fazio, M. Dalmonte, and M. Schirò, Measurement-induced entanglement transitions in the quantum Ising chain: From infinite to zero clicks, *Phys. Rev. B* **103**, 224210 (2021).
- [39] S.-K. Jian, C. Liu, X. Chen, B. Swingle, and P. Zhang, Measurement-Induced Phase Transition in the Monitored Sachdev-Ye-Kitaev Model, *Phys. Rev. Lett.* **127**, 140601 (2021).
- [40] T. Minato, K. Sugimoto, T. Kuwahara, and K. Saito, Fate of Measurement-Induced Phase Transition in Long-Range Interactions, *Phys. Rev. Lett.* **128**, 010603 (2022).
- [41] M. Block, Y. Bao, S. Choi, E. Altman, and N. Y. Yao, Measurement-Induced Transition in Long-Range Interacting Quantum Circuits, *Phys. Rev. Lett.* **128**, 010604 (2022).
- [42] A. Zabalo, M. J. Gullans, J. H. Wilson, R. Vasseur, A. W. W. Ludwig, S. Gopalakrishnan, D. A. Huse, and J. H. Pixley, Operator Scaling Dimensions and Multifractality at Measurement-Induced Transitions, *Phys. Rev. Lett.* **128**, 050602 (2022).
- [43] X. Turkeshi, M. Dalmonte, R. Fazio, and M. Schirò, Entanglement transitions from stochastic resetting of non-Hermitian quasiparticles, *Phys. Rev. B* **105**, L241114 (2022).
- [44] K. Yamamoto and R. Hamazaki, Localization properties in disordered quantum many-body dynamics under continuous measurement, *Phys. Rev. B* **107**, L220201 (2023).
- [45] T.-C. Lu, Z. Zhang, S. Vijay, and T. H. Hsieh, Mixed-State Long-Range Order and Criticality from Measurement and Feedback, *PRX Quantum* **4**, 030318 (2023).
- [46] V. B. Bulchandani, S. L. Sondhi, and J. T. Chalker, Random-Matrix Models of Monitored Quantum Circuits, *J. Stat. Phys.* **191**, 55 (2024).
- [47] A. De Luca, C. Liu, A. Nahum, and T. Zhou, Universality classes for purification in nonunitary quantum processes (2023), arXiv:2312.17744.
- [48] K. Mochizuki and R. Hamazaki, Measurement-Induced Spectral Transition (2024), arXiv:2406.18234.
- [49] C. Noel, P. Niroula, D. Zhu, A. Risinger, L. Egan, D. Biswas, M. Cetina, A. V. Gorshkov, M. J. Gullans, D. A. Huse, and C. Monroe, Measurement-induced quantum phases realized in a trapped-ion quantum computer, *Nat. Phys.* **18**, 760 (2022).
- [50] J. M. Koh, S.-N. Sun, M. Motta, and A. J. Minnich, Measurement-induced entanglement phase transition on a superconducting quantum processor with mid-circuit readout, *Nat. Phys.* **19**, 1314 (2023).
- [51] Google Quantum AI and Collaborators, Measurement-induced entanglement and teleportation on a noisy quantum processor, *Nature* **622**, 481 (2023).
- [52] X. Cao, A. Tilloy, and A. De Luca, Entanglement in a fermion chain under continuous monitoring, *SciPost Phys.* **7**, 024 (2019).
- [53] A. Nahum and B. Skinner, Entanglement and dynamics of diffusion-annihilation processes with Majorana defects, *Phys. Rev. Research* **2**, 023288 (2020).
- [54] X. Chen, Y. Li, M. P. A. Fisher, and A. Lucas, Emergent conformal symmetry in nonunitary random dynamics of free fermions, *Phys. Rev. Research* **2**, 033017 (2020).
- [55] O. Alberton, M. Buchhold, and S. Diehl, Entanglement Transition in a Monitored Free-Fermion Chain: From Extended Criticality to Area Law, *Phys. Rev. Lett.* **126**, 170602 (2021).
- [56] C.-M. Jian, B. Bauer, A. Keselman, and A. W. W. Ludwig, Criticality and entanglement in nonunitary quantum circuits and tensor networks of noninteracting fermions, *Phys. Rev. B* **106**, 134206 (2022).
- [57] Q. Tang, X. Chen, and W. Zhu, Quantum criticality in the nonunitary dynamics of $(2+1)$ -dimensional free fermions, *Phys. Rev. B* **103**, 174303 (2021).
- [58] M. Buchhold, Y. Minoguchi, A. Altland, and S. Diehl, Effective Theory for the Measurement-Induced Phase Transition of Dirac Fermions, *Phys. Rev. X* **11**, 041004 (2021).
- [59] T. Müller, S. Diehl, and M. Buchhold, Measurement-Induced Dark State Phase Transitions in Long-Ranged Fermion Systems, *Phys. Rev. Lett.* **128**, 010605 (2022).
- [60] M. Coppola, E. Tirrito, D. Karevski, and M. Collura, Growth of entanglement entropy under local projective measurements, *Phys. Rev. B* **105**, 094303 (2022).

- [61] G. Kells, D. Meidan, and A. Romito, Topological transitions in weakly monitored free fermions, *SciPost Phys.* **14**, 031 (2023).
- [62] C. Fleckenstein, A. Zorzato, D. Varjas, E. J. Bergholtz, J. H. Bardarson, and A. Tiwari, Non-Hermitian topology in monitored quantum circuits, *Phys. Rev. Research* **4**, L032026 (2022).
- [63] K. Kawabata, T. Numasawa, and S. Ryu, Entanglement Phase Transition Induced by the Non-Hermitian Skin Effect, *Phys. Rev. X* **13**, 021007 (2023).
- [64] Y.-P. Wang, C. Fang, and J. Ren, Absence of measurement-induced entanglement transition due to feedback-induced skin effect, *Phys. Rev. B* **110**, 035113 (2024).
- [65] J. Merritt and L. Fidkowski, Entanglement transitions with free fermions, *Phys. Rev. B* **107**, 064303 (2023).
- [66] Y. Le Gal, X. Turkeshi, and M. Schirò, Volume-to-area law entanglement transition in a non-Hermitian free fermionic chain, *SciPost Phys.* **14**, 138 (2023).
- [67] M. Sznyszewski, O. Lunt, and A. Pal, Disordered monitored free fermions, *Phys. Rev. B* **108**, 165126 (2023).
- [68] C.-M. Jian, H. Shapourian, B. Bauer, and A. W. W. Ludwig, Measurement-induced entanglement transitions in quantum circuits of non-interacting fermions: Born-rule versus forced measurements (2023), arXiv:2302.09094.
- [69] T. Swann, D. Bernard, and A. Nahum, Spacetime picture for entanglement generation in noisy fermion chains (2023), arXiv:2302.12212.
- [70] M. Fava, L. Piroli, T. Swann, D. Bernard, and A. Nahum, Nonlinear Sigma Models for Monitored Dynamics of Free Fermions, *Phys. Rev. X* **13**, 041045 (2023).
- [71] H. Lóio, A. De Luca, J. De Nardis, and X. Turkeshi, Purification timescales in monitored fermions, *Phys. Rev. B* **108**, L020306 (2023).
- [72] I. Poboiko, P. Pöpperl, I. V. Gornyi, and A. D. Mirlin, Theory of Free Fermions under Random Projective Measurements, *Phys. Rev. X* **13**, 041046 (2023).
- [73] K. Chahine and M. Buchhold, Entanglement phases, localization, and multifractality of monitored free fermions in two dimensions, *Phys. Rev. B* **110**, 054313 (2024).
- [74] I. Poboiko, I. V. Gornyi, and A. D. Mirlin, Measurement-Induced Phase Transition for Free Fermions above One Dimension, *Phys. Rev. Lett.* **132**, 110403 (2024).
- [75] Z.-C. Liu, K. Li, and Y. Xu, Dynamical Transition Due to Feedback-Induced Skin Effect, *Phys. Rev. Lett.* **133**, 090401 (2024).
- [76] M. Fava, L. Piroli, D. Bernard, and A. Nahum, A tractable model of monitored fermions with conserved $U(1)$ charge (2024), arXiv:2407.08045.
- [77] Z. Xiao, T. Ohtsuki, and K. Kawabata, Universal Stochastic Equations of Monitored Quantum Dynamics (2024), arXiv:2408.16974.
- [78] P. W. Anderson, Absence of Diffusion in Certain Random Lattices, *Phys. Rev.* **109**, 1492 (1958).
- [79] E. Abrahams, P. W. Anderson, D. C. Licciardello, and T. V. Ramakrishnan, Scaling Theory of Localization: Absence of Quantum Diffusion in Two Dimensions, *Phys. Rev. Lett.* **42**, 673 (1979).
- [80] P. A. Lee and T. V. Ramakrishnan, Disordered electronic systems, *Rev. Mod. Phys.* **57**, 287 (1985).
- [81] C. W. J. Beenakker, Random-matrix theory of quantum transport, *Rev. Mod. Phys.* **69**, 731 (1997).
- [82] F. Evers and A. D. Mirlin, Anderson transitions, *Rev. Mod. Phys.* **80**, 1355 (2008).
- [83] R. E. Prange and S. M. Girvin, eds., *The Quantum Hall Effect* (Springer, New York, 1987).
- [84] B. Huckestein, Scaling theory of the integer quantum Hall effect, *Rev. Mod. Phys.* **67**, 357 (1995).
- [85] B. Kramer, T. Ohtsuki, and S. Kettemann, Random network models and quantum phase transitions in two dimensions, *Phys. Rep.* **417**, 211 (2005).
- [86] A. P. Schnyder, S. Ryu, A. Furusaki, and A. W. W. Ludwig, Classification of topological insulators and superconductors in three spatial dimensions, *Phys. Rev. B* **78**, 195125 (2008).
- [87] A. Kitaev, Periodic table for topological insulators and superconductors, *AIP Conf. Proc.* **1134**, 22 (2009).
- [88] S. Ryu, A. P. Schnyder, A. Furusaki, and A. W. W. Ludwig, Topological insulators and superconductors: tenfold way and dimensional hierarchy, *New J. Phys.* **12**, 065010 (2010).
- [89] M. Z. Hasan and C. L. Kane, Colloquium: Topological insulators, *Rev. Mod. Phys.* **82**, 3045 (2010).
- [90] X.-L. Qi and S.-C. Zhang, Topological insulators and superconductors, *Rev. Mod. Phys.* **83**, 1057 (2011).
- [91] C.-K. Chiu, J. C. Y. Teo, A. P. Schnyder, and S. Ryu, Classification of topological quantum matter with symmetries, *Rev. Mod. Phys.* **88**, 035005 (2016).
- [92] D. Bernard and A. LeClair, A Classification of Non-Hermitian Random Matrices, in *Statistical Field Theories*, edited by A. Cappelli and G. Mussardo (Springer, Dordrecht, 2002) pp. 207–214.
- [93] K. Kawabata, K. Shiozaki, M. Ueda, and M. Sato, Symmetry and Topology in Non-Hermitian Physics, *Phys. Rev. X* **9**, 041015 (2019).
- [94] M. R. Zirnbauer, Riemannian symmetric superspaces and their origin in random-matrix theory, *J. Math. Phys.* **37**, 4986 (1996).
- [95] S. Bravyi, Lagrangian representation for fermionic linear optics, *Quantum Inf. Comput.* **5**, 216 (2005).
- [96] K. Jacobs and D. A. Steck, A straightforward introduction to continuous quantum measurement, *Contemp. Phys.* **47**, 279 (2006).
- [97] H. M. Wiseman and G. J. Milburn, *Quantum Measurement and Control* (Cambridge University Press, Cambridge, England, 2009).
- [98] See the Supplemental Material for classification of single-particle Kraus operators and numerical details on monitored free fermions in $0 + 1$, $1 + 1$, and $2 + 1$ dimensions.
- [99] A. Altland and M. R. Zirnbauer, Nonstandard symmetry classes in mesoscopic normal-superconducting hybrid structures, *Phys. Rev. B* **55**, 1142 (1997).
- [100] Z. Gong, Y. Ashida, K. Kawabata, K. Takasan, S. Hishikawa, and M. Ueda, Topological Phases of Non-Hermitian Systems, *Phys. Rev. X* **8**, 031079 (2018).
- [101] M. Karoubi, *K-Theory: An Introduction* (Springer, Berlin, Heidelberg, 1978).
- [102] S. Lieu, M. McGinley, and N. R. Cooper, Tenfold Way for Quadratic Lindbladians, *Phys. Rev. Lett.* **124**, 040401 (2020).
- [103] A. Altland, M. Fleischhauer, and S. Diehl, Symmetry Classes of Open Fermionic Quantum Matter, *Phys. Rev. X* **11**, 021037 (2021).

- [104] L. Sá, P. Ribeiro, and T. Prosen, Symmetry Classification of Many-Body Lindbladians: Tenfold Way and Beyond, *Phys. Rev. X* **13**, 031019 (2023).
- [105] K. Kawabata, A. Kulkarni, J. Li, T. Numasawa, and S. Ryu, Symmetry of Open Quantum Systems: Classification of Dissipative Quantum Chaos, *PRX Quantum* **4**, 030328 (2023).
- [106] M. Nakagawa and M. Ueda, Topology of Discrete Quantum Feedback Control (2024), arXiv:2403.08406.
- [107] F. J. Dyson, The Dynamics of a Disordered Linear Chain, *Phys. Rev.* **92**, 1331 (1953).
- [108] P. W. Brouwer, C. Mudry, B. D. Simons, and A. Altland, Delocalization in Coupled One-Dimensional Chains, *Phys. Rev. Lett.* **81**, 862 (1998).
- [109] I. Mondragon-Shem, T. L. Hughes, J. Song, and E. Prodan, Topological Criticality in the Chiral-Symmetric AIII Class at Strong Disorder, *Phys. Rev. Lett.* **113**, 046802 (2014).
- [110] A. Altland, D. Bagrets, L. Fritz, A. Kamenev, and H. Schmiedt, Quantum Criticality of Quasi-One-Dimensional Topological Anderson Insulators, *Phys. Rev. Lett.* **112**, 206602 (2014).
- [111] N. Hatano and D. R. Nelson, Localization Transitions in Non-Hermitian Quantum Mechanics, *Phys. Rev. Lett.* **77**, 570 (1996).
- [112] N. Hatano and D. R. Nelson, Vortex pinning and non-Hermitian quantum mechanics, *Phys. Rev. B* **56**, 8651 (1997).
- [113] H. Furstenberg and H. Kesten, Products of Random Matrices, *Ann. Math. Statist.* **31**, 457 (1960).
- [114] A. Y. Kitaev, Unpaired Majorana fermions in quantum wires, *Phys.-Usp.* **44**, 131 (2001).
- [115] J. D. Hannukainen, M. F. Martínez, J. H. Bardarson, and T. K. Kivring, Local Topological Markers in Odd Spatial Dimensions and Their Application to Amorphous Topological Matter, *Phys. Rev. Lett.* **129**, 277601 (2022).
- [116] S. Hikami, Three-loop β -functions of non-linear σ models on symmetric spaces, *Phys. Lett. B* **98**, 208 (1981).
- [117] F. Wegner, Four-loop-order β -function of nonlinear σ -models in symmetric spaces, *Nucl. Phys. B* **316**, 663 (1989).
- [118] T. Wang, Z. Pan, K. Slevin, and T. Ohtsuki, Critical behavior of the Anderson transition in higher-dimensional Bogoliubov–de Gennes symmetry classes, *Phys. Rev. B* **108**, 144208 (2023).
- [119] Z. Xiao *et al.* (in preparation).
- [120] P. G. Harper, Single Band Motion of Conduction Electrons in a Uniform Magnetic Field, *Proc. Phys. Soc. A* **68**, 874 (1955).
- [121] E. Prodan, T. L. Hughes, and B. A. Bernevig, Entanglement Spectrum of a Disordered Topological Chern Insulator, *Phys. Rev. Lett.* **105**, 115501 (2010).
- [122] H. Pan, H. Shapourian, and C.-M. Jian, Topological Modes in Monitored Quantum Dynamics (2024), arXiv:2411.04191.
- [123] T. E. Lee, Anomalous Edge State in a Non-Hermitian Lattice, *Phys. Rev. Lett.* **116**, 133903 (2016).
- [124] S. Yao and Z. Wang, Edge States and Topological Invariants of Non-Hermitian Systems, *Phys. Rev. Lett.* **121**, 086803 (2018).
- [125] F. K. Kunst, E. Edvardsson, J. C. Budich, and E. J. Bergholtz, Biorthogonal Bulk-Boundary Correspondence in Non-Hermitian Systems, *Phys. Rev. Lett.* **121**, 026808 (2018).
- [126] K. Yokomizo and S. Murakami, Non-Bloch Band Theory of Non-Hermitian Systems, *Phys. Rev. Lett.* **123**, 066404 (2019).
- [127] K. Zhang, Z. Yang, and C. Fang, Correspondence between Winding Numbers and Skin Modes in Non-Hermitian Systems, *Phys. Rev. Lett.* **125**, 126402 (2020).
- [128] N. Okuma, K. Kawabata, K. Shiozaki, and M. Sato, Topological Origin of Non-Hermitian Skin Effects, *Phys. Rev. Lett.* **124**, 086801 (2020).
- [129] G. Lee, T. Jin, Y.-X. Wang, A. McDonald, and A. Clerk, Entanglement Phase Transition Due to Reciprocity Breaking without Measurement or Postselection, *PRX Quantum* **5**, 010313 (2024).
- [130] H. Oshima, K. Mochizuki, R. Hamazaki, and Y. Fuji (in preparation).

Supplemental Material for “Topology of Monitored Quantum Dynamics”

Zhenyu Xiao^{1,*} and Kohei Kawabata^{2,†}

¹*International Center for Quantum Materials, Peking University, Beijing 100871, China*

²*Institute for Solid State Physics, University of Tokyo, Kashiwa, Chiba 277-8581, Japan*

(Dated: December 10, 2024)

CONTENTS

I. Classification of single-particle Kraus operators	1
II. Topology of L_t and \bar{H}_t	2
A. Class A	2
B. Class AIII	2
III. Monitored complex fermions in $0 + 1$ dimension	3
IV. Monitored Majorana fermions in $1 + 1$ dimensions	4
A. Models	4
B. Numerical details	5
C. Local topological markers	5
V. Monitored complex fermions in $2 + 1$ dimensions	5
References	6

I. CLASSIFICATION OF SINGLE-PARTICLE KRAUS OPERATORS

As discussed in the main text, within the 38-fold symmetry classification of non-Hermitian operators [1], symmetries relevant to single-particle Kraus operators K_t are

$$\mathcal{T}K_t^*\mathcal{T}^{-1} = K_t, \quad \mathcal{C}(K_t^T)^{-1}\mathcal{C}^{-1} = K_t, \quad \Gamma(K_t^\dagger)^{-1}\Gamma^{-1} = K_t, \quad (\text{S1})$$

with unitary operators \mathcal{T} , \mathcal{C} , and Γ satisfying $\mathcal{T}\mathcal{T}^* = \pm 1$, $\mathcal{C}\mathcal{C}^* = \pm 1$, and $\Gamma^2 = 1$, respectively. Consequently, K_t is associated with the tenfold classifying spaces in Table I of the main text, corresponding to noncompact types (see,

Supplementary Table 1. Tenfold topological classification of single-particle Kraus operators K in d spatial dimensions and one temporal dimension. The classification reduces to the point-gap topology in the Altland-Zirnbauer[†] symmetry class [1].

Symmetry		$d + 1 = 1$	$d + 1 = 2$	$d + 1 = 3$	$d + 1 = 4$	$d + 1 = 5$	$d + 1 = 6$	$d + 1 = 7$	$d + 1 = 8$
A	\mathcal{C}_1	\mathbb{Z}	0	\mathbb{Z}	0	\mathbb{Z}	0	\mathbb{Z}	0
AIII	\mathcal{C}_0	0	\mathbb{Z}	0	\mathbb{Z}	0	\mathbb{Z}	0	\mathbb{Z}
AI	\mathcal{R}_7	0	0	$2\mathbb{Z}$	0	\mathbb{Z}_2	\mathbb{Z}_2	\mathbb{Z}	0
BDI	\mathcal{R}_0	0	0	0	$2\mathbb{Z}$	0	\mathbb{Z}_2	\mathbb{Z}_2	\mathbb{Z}
D	\mathcal{R}_1	\mathbb{Z}	0	0	0	$2\mathbb{Z}$	0	\mathbb{Z}_2	\mathbb{Z}_2
DIII	\mathcal{R}_2	\mathbb{Z}_2	\mathbb{Z}	0	0	0	$2\mathbb{Z}$	0	\mathbb{Z}_2
AII	\mathcal{R}_3	\mathbb{Z}_2	\mathbb{Z}_2	\mathbb{Z}	0	0	0	$2\mathbb{Z}$	0
CII	\mathcal{R}_4	0	\mathbb{Z}_2	\mathbb{Z}_2	\mathbb{Z}	0	0	0	$2\mathbb{Z}$
C	\mathcal{R}_5	$2\mathbb{Z}$	0	\mathbb{Z}_2	\mathbb{Z}_2	\mathbb{Z}	0	0	0
CI	\mathcal{R}_6	0	$2\mathbb{Z}$	0	\mathbb{Z}_2	\mathbb{Z}_2	\mathbb{Z}	0	0

* wjkxzy@pku.edu.cn

† kawabata@issp.u-tokyo.ac.jp

for example, Table I in Ref. [2] and Table IV in Ref. [3]). Notably, these classifying spaces also coincide with those of point-gapped non-Hermitian systems in the Altland-Zirnbauer[†] symmetry class [1]. In Table 1, we provide the tenfold topological classification of single-particle Kraus operators K_t , constituting a different tenfold way from that of non-Hermitian dynamical generators L_t shown in Table II of the main text. From the homotopy perspective, topology is characterized by $\pi_0(\mathcal{C}_{s-(d+1)})$ or $\pi_0(\mathcal{R}_{s-(d+1)})$, which obey $\mathcal{C}_{s+2} \cong \mathcal{C}_s$ and $\mathcal{R}_{s+8} \cong \mathcal{R}_s$ due to the Bott periodicity in K -theory [4].

II. TOPOLOGY OF L_t AND \bar{H}_t

As discussed in the main text, $L_t := \partial_t - H_t$ is a non-Hermitian operator acting on $(d+1)$ -dimensional spacetime, while \bar{H}_t , defined by $K_{[0,t]} := e^{\bar{H}_t t}$, represents the time average of H_t and acts on d -dimensional space. We assume that the temporal fluctuations of \bar{H}_t are negligible for $t \rightarrow \infty$, leading to $\bar{H}_t = \bar{H}$, independent of time. In the subsequent discussion on topological invariants, we further assume (spatial) translation invariance of \bar{H} for convenience, and its Bloch Hamiltonian is denoted by $\bar{H}(\mathbf{k})$. In this case, the Fourier transform of L_t is given by $L(\omega, \mathbf{k}) = i\omega - \bar{H}(\mathbf{k})$, equivalent to the inverse of the Green's function, $G^{-1}(i\omega, \mathbf{k}) := i\omega - \bar{H}(\mathbf{k})$.

A. Class A

In class A and $2n$ spatial dimensions ($n \in \mathbb{Z}$), $\bar{H}(\mathbf{k})$ is characterized by the n th Chern number C_n in the presence of a real line gap with respect to $\text{Re } z = 0$. Meanwhile, $L(\omega, \mathbf{k})$ belongs to class A and acts on $2n+1$ dimensions, whose point-gap topology is characterized by the $(2n+1)$ -dimensional winding number W_{2n+1} . Both invariants coincide with each other, given as [1, 5]

$$C_n = W_{2n+1} = \frac{n!}{(2\pi i)^{n+1} (2n+1)!} \int_{(\omega, \mathbf{k})} \text{Tr} (L dL^{-1})^{2n+1}, \quad (\text{S2})$$

which represents the correspondence of topology between \bar{H} and L_t in class A.

B. Class AIII

In class AIII and $2n-1$ spatial dimensions ($n \in \mathbb{Z}$), $\bar{H}(\mathbf{k})$ is characterized by the $(2n-1)$ -dimensional winding number W_{2n-1} in the presence of a real line gap with respect to $\text{Re } z = 0$. Without loss of generality, let the chiral operator for \bar{H} be a Pauli matrix σ_z , i.e., $\sigma_z \bar{H}(\mathbf{k}) \sigma_z = -\bar{H}(\mathbf{k})$. Due to the real line gap, $\bar{H}(\mathbf{k})$ can be continuously deformed into a flat-band Hermitian Hamiltonian $h(\mathbf{k})$ in class AIII:

$$h(\mathbf{k}) = P(\mathbf{k}) \begin{pmatrix} 1_{p \times p} & 0 \\ 0 & -1_{p \times p} \end{pmatrix} P^\dagger(\mathbf{k}), \quad (\text{S3})$$

where $2p$ is the number of the bands, and P is a unitary matrix ($PP^\dagger = P^\dagger P = 1$). Due to chiral symmetry, $P(\mathbf{k})$ takes the form of

$$P(\mathbf{k}) = \frac{1}{\sqrt{2}} \begin{pmatrix} U(\mathbf{k}) & U(\mathbf{k}) \\ V(\mathbf{k}) & -V(\mathbf{k}) \end{pmatrix}, \quad (\text{S4})$$

with unitary matrices U and V , leading to

$$h(\mathbf{k}) = \begin{pmatrix} 0 & U(\mathbf{k})V^\dagger(\mathbf{k}) \\ V(\mathbf{k})U^\dagger(\mathbf{k}) & 0 \end{pmatrix}. \quad (\text{S5})$$

Introducing $Q(\mathbf{k}) := U(\mathbf{k})V^\dagger(\mathbf{k})$, we have the $(2n-1)$ -dimensional winding number

$$W_{2n-1} = \frac{(n-1)!}{(2\pi i)^n (2n-1)!} \int_{\mathbf{k}} \text{Tr} (Q dQ^{-1})^{2n-1}, \quad (\text{S6})$$

where $\int_{\mathbf{k}}$ denotes the integral over $(2n-1)$ -dimensional momentum space.

On the other hand, $L(\omega, \mathbf{k})$ belongs to class AIII and acts on $2n$ dimensions, whose point-gap topology is characterized by the n th Chern number C_n , as explained below. As discussed in the main text, we introduce a Hermitized operator

$$\tilde{L}(\omega, \mathbf{k}) := \begin{pmatrix} 0 & L(\omega, \mathbf{k}) \\ L^\dagger(\omega, \mathbf{k}) & 0 \end{pmatrix}, \quad (\text{S7})$$

sharing the same topological classification with $L(\omega, \mathbf{k})$. Owing to chiral symmetry of $H(\mathbf{k})$, $L(\omega, \mathbf{k}) = i\omega - \bar{H}(\mathbf{k})$ also respects chiral symmetry $\sigma_z L^\dagger(\omega, \mathbf{k}) \sigma_z = -L(\omega, \mathbf{k})$. Consequently, after a unitary transformation, $\tilde{L}(\omega, \mathbf{k})$ can be block diagonalized into

$$\begin{pmatrix} \tilde{l}(\omega, \mathbf{k}) & 0 \\ 0 & -\tilde{l}(\omega, \mathbf{k}) \end{pmatrix}, \quad \tilde{l}(\omega, \mathbf{k}) := -iL(\omega, \mathbf{k})\sigma_z = \omega\sigma_z + i\bar{H}(\mathbf{k})\sigma_z. \quad (\text{S8})$$

Then, the topological classification of $L(\omega, \mathbf{k})$ reduces to that of the Hermitian matrix $\tilde{l}(\omega, \mathbf{k})$ in class A, classified by the n th Chern number C_n . Through the continuous deformation from $\bar{H}(\mathbf{k})$ to $h(\mathbf{k})$, the energy gap remains open, and we can continuously deform $\tilde{l}(\omega, \mathbf{k})$ to $l(\omega, \mathbf{k}) := \omega\sigma_z + ih(\mathbf{k})\sigma_z$. Therefore, $\tilde{l}(\omega, \mathbf{k})$ and $l(\omega, \mathbf{k})$ share the same Chern number. In addition, $l(\omega, \mathbf{k})$ is diagonalized as

$$l(\omega, \mathbf{k}) = \mathcal{U} \begin{pmatrix} \sqrt{1+\omega^2} & 0 \\ 0 & -\sqrt{1+\omega^2} \end{pmatrix} \mathcal{U}^\dagger \text{ with } \mathcal{U} := \frac{1}{\sqrt{1+y^2}} \begin{pmatrix} U & iyU \\ iyV & V \end{pmatrix} \text{ and } y := \sqrt{1+\omega^2} - \omega. \quad (\text{S9})$$

Furthermore, l is continuously deformable into the flat-band Hamiltonian \mathcal{Q} ,

$$\mathcal{Q} := \mathcal{U} \begin{pmatrix} 1 & 0 \\ 0 & -1 \end{pmatrix} \mathcal{U}^\dagger = \frac{1}{\sqrt{1+\omega^2}} \begin{pmatrix} \omega & -iQ \\ iQ^\dagger & -\omega \end{pmatrix}. \quad (\text{S10})$$

Then, the n th Chern number C_n is given as

$$C_n = -\frac{1}{2^{2n+1}n!} \left(\frac{i}{2\pi}\right)^n \int_{(\omega, \mathbf{k})} \text{Tr} \left[\mathcal{Q} (d\mathcal{Q})^{2n} \right]. \quad (\text{S11})$$

Notably, we have $C_n = -W_{2n-1}$. As an illustration, let us consider $n = 1$. Using $k_0 := \omega$, $\mathbf{k} := (k_1, k_2, \dots, k_{2n-1})$, and $\partial_i := \frac{\partial}{\partial k_i}$ ($i = 0, 1, 2, \dots, 2n-1$), we have

$$\partial_0 \mathcal{Q} = \frac{1}{(1+\omega^2)^{3/2}} \begin{pmatrix} 1 & i\omega Q \\ -i\omega Q^\dagger & -1 \end{pmatrix}, \quad \partial_i \mathcal{Q} = \frac{1}{\sqrt{1+\omega^2}} \begin{pmatrix} 0 & -i\partial_i Q \\ i\partial_i Q^\dagger & 0 \end{pmatrix} \quad (i \neq 0). \quad (\text{S12})$$

Then, we have for $n = 1$

$$\begin{aligned} C_1 &= -\frac{i}{16\pi} \int \text{Tr}(\mathcal{Q}\partial_0\mathcal{Q}\partial_1\mathcal{Q} - \mathcal{Q}\partial_1\mathcal{Q}\partial_0\mathcal{Q})d\omega dk_1 \\ &= \frac{i}{16\pi} \int \frac{4}{(1+\omega^2)^{3/2}}d\omega \int \text{Tr}(Q\partial_1Q^{-1})dk_1 \\ &= -\frac{1}{2\pi i} \int \text{Tr}(Q\partial_1Q^{-1})dk_1, \end{aligned} \quad (\text{S13})$$

identical to $-W_1$ in Eq. S6.

III. MONITORED COMPLEX FERMIONS IN 0 + 1 DIMENSION

We generally formulate the \mathbb{Z} topological invariant for non-Hermitian dynamical generators L_t in 0 + 1 spacetime dimension. We introduce a U(1) scalar potential μ and assume that $L_t = L_t(\mu)$ remains invertible for arbitrary μ , i.e.,

$$\forall \mu \in \mathbb{R} \quad \det L_t(\mu) \neq 0. \quad (\text{S14})$$

This condition corresponds to the presence of a point gap for non-Hermitian operators L_t [1, 6]. While the complex spectrum of L_t generally depends on μ , it remains invariant under the insertion of a unit scalar potential $\mu = 2\pi$.

Consequently, the winding number W_1 of the determinant of L_t in the complex plane is well defined under the adiabatic cycle of the unit scalar potential:

$$W_1 := \oint_0^{2\pi} \frac{d\mu}{2\pi i} \frac{d}{d\mu} \log \det L_t(\mu). \quad (\text{S15})$$

This expression gives the \mathbb{Z} topological invariant for $d+1=1$ and class A in Table II of the main text.

While L_t is inherently stochastic, let us suppose that L_t is invariant under time translation. Under this condition, we can perform its Fourier transform $\tilde{L}(\omega)$, leading to

$$W_1 := - \oint_{-\infty}^{\infty} \frac{d\omega}{2\pi i} \frac{d}{d\omega} \log \det \tilde{L}(\omega). \quad (\text{S16})$$

For example, for $L_t = \partial_t - \gamma$, its Fourier transform becomes $\tilde{L}(\omega) = i\omega - \gamma$, yielding $W_1 = \text{sgn}(\gamma)/2$. Notably, this winding number W_1 also coincides with the zeroth Chern number of $H_t = \partial_t - L_t = \gamma$, consistent with Sec. II.

To clarify nontrivial topology in zero spatial dimension $d=0$, we consider the random nonunitary quantum dynamics of N complex fermions whose particle numbers n_i 's ($i=1, \dots, N$) are continuously measured. The associated non-Hermitian dynamical generator L_t is expressed as [7–9]

$$L_t = \partial_t + ih_t - \gamma(2\langle n \rangle_t - 1) - \sqrt{\gamma}w_t, \quad (\text{S17})$$

where h_t denotes a random time-dependent $N \times N$ Hermitian Hamiltonian, $\gamma > 0$ the measurement strength, $\langle n \rangle_t := \text{diag}(\langle n_1 \rangle_t, \dots, \langle n_N \rangle_t)$ the average particle numbers, and w_t a stochastic noise term. Since L_t respects no internal symmetry, it falls into class A and exhibits \mathbb{Z} topology (see Tables I and II in the main text). As discussed above, the corresponding \mathbb{Z} topological invariant is the winding number W_1 of the complex spectrum of L_t during the adiabatic insertion of the U(1) scalar potential, reducing to $W_1 = \sum_{i=1}^N \text{sgn}(\langle n_i \rangle_t - 1/2)/2$ on average.

As shown in Ref. [9], Born measurements inherently drive the average particle numbers to $\langle n_i \rangle_t = 0$ or $\langle n_i \rangle_t = 1$ for $t \rightarrow \infty$, yielding a topological mass term accompanied by the exponential decay of entropy. By contrast, forced measurements can stabilize a special mode with $\langle n_i \rangle_t = 1/2$, leading to critical behavior with a divergent purification time. We find that this quantum criticality is protected by the \mathbb{Z} topology, akin to disordered quantum wires with chiral symmetry [10–13]. Notably, it also shares the same universality class as the Anderson transitions induced by point-gap topology in nonreciprocal disordered systems; upon replacing time with space, L_t becomes a continuum counterpart of the Hatano-Nelson model [14, 15].

IV. MONITORED MAJORANA FERMIONS IN 1 + 1 DIMENSIONS

A. Models

We consider circuit models of a monitored single Majorana chain (Fig. 1 in the main text). There exists one Majorana operator ψ_i ($i=1, 2, \dots, L$) at each site, satisfying $\psi_i = \psi_i^\dagger$ and $\{\psi_i, \psi_j\} = 2\delta_{ij}$. At $t=1$, the odd pairs $i\psi_{2i-1}\psi_{2i}$'s ($i=1, 2, \dots, L/2$) are measured with strength $\Gamma_o = \Gamma(1 + \Delta)$, given by the Kraus operators $K_{2i-1, \pm} = (2 \cosh \Gamma_o)^{-1} e^{\pm i\Gamma_o \psi_{2i-1}\psi_{2i}/2}$ with \pm specifying the measurement results. Under Born measurement, a Kraus operator K_{\pm} transforms a density matrix ρ_0 to $\frac{K_{\pm}\rho_0 K_{\pm}^\dagger}{\text{Tr}(K_{\pm}\rho_0 K_{\pm}^\dagger)}$ with probability $\text{Tr}(K_{\pm}\rho_0 K_{\pm}^\dagger)$. At $t=2$, the even pairs $i\psi_{2i}\psi_{2i+1}$'s are measured with strength $\Gamma_e = \Gamma(1 - \Delta)$, given by the Kraus operators $K_{2i, \pm} = (2 \cosh \Gamma_e)^{-1} e^{\pm i\Gamma_e \psi_{2i}\psi_{2i+1}/2}$. Repeating the measurements at $t=1$ and $t=2$ generates the measurement-only dynamics of a single Majorana chain. At $t=3$, random unitary operations $U_{2i-1} = e^{\theta_{2i-1}\psi_{2i-1}\psi_{2i}/2}$ ($i=1, 2, \dots, L/2$) are applied. At $t=4$, $U_{2i} = e^{\theta_{2i}\psi_{2i}\psi_{2i+1}/2}$ are applied. The real random variables θ_i 's are distributed uniformly and independently in $[-W/2, W/2]$ ($W \geq 0$). Repeating the operations from $t=1$ to $t=4$ generates generic monitored dynamics of Majorana fermions.

Let e^H be the single-particle representation of $K_{2i-1, +}$: $H_{jk} = i\Gamma_o(\delta_{j,2i-1}\delta_{k,2i} - \delta_{j,2i}\delta_{k,2i-1})$ in the basis $(\psi_1, \psi_2, \dots, \psi_L)$. The $L \times L$ matrix H satisfies particle-hole symmetry $H = -H^T$ and chiral symmetry $H = -\Gamma H^\dagger \Gamma^{-1}$ with $\Gamma_{jk} = \delta_{jk}(-1)^j$, and hence belongs to class BDI. Similarly, the single-particle representations of $K_{2i-1, -}$ and $K_{2i, \pm}$ respect particle-hole symmetry and chiral symmetry with the same choice of Γ . Thus, the measurement-only dynamics belongs to class BDI. By contrast, the single-particle representation of $U_i = e^{\theta_i \psi_i \psi_{i+1}/2}$ is $e^{H'}$ with $(H')_{jk} = \theta(\delta_{j,i}\delta_{k,i+1} - \delta_{j,i+1}\delta_{k,i})$. Since we have $H' = -(H')^T$ but $H' = \Gamma(H')^\dagger \Gamma^{-1}$, H' respects particle-hole symmetry but breaks chiral symmetry. Thus, the generic monitored dynamics belongs to class D.

Next, we consider circuit models of monitored double Majorana chains. At each site, there exist two Majorana operators ψ_i^A and ψ_i^B with A and B being the chain indices. The dynamics is generated by repeating the operations

previously discussed for individual chains (the operations at $t = 1$ and $t = 2$ for class BDI and at $t = 1, 2, 3, 4$ for class D) along with the unitary gates. The unitary gates $e^{\phi_i \psi_i^A \psi_i^B / 2}$ ($i = 1, 2, \dots, L$) with ϕ_i 's distributed uniformly and independently in $[-W'/2, W'/2]$. Let e^{H_c} be the single-particle representation of $e^{\phi_i \psi_i^A \psi_i^B / 2}$. It can be verified that H_c satisfies $H_c = -\Gamma(H_c)^\dagger \Gamma^{-1}$, where Γ is chosen as $\Gamma_{j\alpha, k\beta} = \delta_{jk} \delta_{\alpha\beta} (-1)^j$ with $\alpha, \beta = A, B$ being the chain indices and $j, k = 1, 2, \dots, L$ being the site indices. Thus, the two measurement-only Majorana chains with such unitary coupling still belong to class BDI.

B. Numerical details

The parameters for the numerical simulations are chosen as $\Delta = \pm 0.8$, $\Gamma = 1$, and $W = 0.4$. Additionally, the system size L ranges from 32 to 256. For the double Majorana chains, we have $W' = 1$, and L ranges from 32 to 128. The evolution time is set to 10^4 cycles. The initial state is chosen as a pure state $|\Psi_0\rangle$ with the correlation function $\langle \Psi_0 | i\psi_{2i-1} \psi_{2i} | \Psi_0 \rangle = 1$ ($i = 1, 2, \dots, L/2$).

We describe the numerical algorithm for a single Majorana chain, which can also be applied to a double chain. The initial state $|\Psi_0\rangle$ is annihilated by the operators $c_n = \frac{1}{\sqrt{2}} \sum_{i=1}^L \psi_i U_{in}$ ($n = 1, 2, \dots, L/2$) with $U = 1_{L/2 \times L/2} \otimes \frac{1}{\sqrt{2}} \begin{pmatrix} 1 \\ -i \end{pmatrix}$. After the application of a Kraus operator with single-particle representation K_1 , the state evolves to $|\Psi_1\rangle$, which is annihilated by $c'_n = \frac{1}{\sqrt{2}} \sum_{i=1}^L \psi_i (K_1 U)_{in}$. We then perform the QR decomposition on $K_1 U$: $K_1 U = U_1 R_1$, where the $L \times L/2$ matrix U_1 satisfies $U_1^\dagger U_1 = 1_{L/2 \times L/2}$ and R is an upper triangular matrix. The state $|\Psi_1\rangle$ should also be annihilated by $c''_n = \sum_{i=1}^L \psi_i (U_1)_{in}$. The correlation function of the updated state is $\langle \Psi_1 | i[\psi_i, \psi_j] | \Psi_1 \rangle = (-2i U_1 U_1^\dagger)_{ij} + i\delta_{ij}$, which determines the Born probability of the Kraus operator to be applied at the next time step. This procedure of the QR decomposition and evaluation of the correlation function is repeated after every action of Kraus operators K_1, K_2, \dots, K_N . The evolution is then expressed as $K_N \dots K_1 U = U_N R_N R_{N-1} \dots R_1$. For $N \gg 1$, the Lyapunov exponent is given as $\eta_i = 1/N \sum_{j=1}^N (R_j)_{ii}$ ($i = 1, 2, \dots, L/2$). Due to particle-hole symmetry, the remaining $L/2$ Lyapunov exponents are $\eta_{L+1-i} = -\eta_i$.

C. Local topological markers

We discuss the formalism of local topological markers [12, 16]. Due to symmetry of the Kraus operators, at each time t , the correlation matrix $(D_t)_{ij} := \langle \Psi_t | i[\psi_i, \psi_j] | \Psi_t \rangle$ is a Hermitian matrix in class BDI (D) for the monitored dynamics in each symmetry class. For the single Majorana chain in class BDI, the chiral-symmetry operator is $\Gamma_{ij} = (-1)^j \delta_{ij}$. To formulate local topological markers, the position operator X should commute with Γ . Thus, we put $(2i-1)$ th site and $(2i)$ th site in one unit cell, and hence the position operator reads $X_{ij} = [i/2] \delta_{ij}$, commuting with Γ . The local chiral index $\nu_{\mathbb{Z}}(x)$ at the x th unit cell is

$$\nu_{\mathbb{Z}}(x) = \sum_{i=2x-1}^{2x} (D_t \Gamma X D_t)_{ii}. \quad (\text{S18})$$

For the single Majorana chain in class D, the correlation function D_t does not respect chiral symmetry. We should instead define a chiral correlation function Q [16] as

$$Q = \frac{1}{2} (D_t + i|[D_t, \Gamma]|^{-1} [D_t, \Gamma]). \quad (\text{S19})$$

Replacing D_t by Q in the formula in Eq. (S18) for $\nu_{\mathbb{Z}}(x)$, we have the local \mathbb{Z}_2 index as $\nu_{\mathbb{Z}_2}(x) \equiv \nu_{\mathbb{Z}}(x) \pmod{2}$.

V. MONITORED COMPLEX FERMIONS IN 2 + 1 DIMENSIONS

We study a circuit model of monitored complex fermions in 2 + 1 dimensions on a square lattice (Fig. S1). Each site $\mathbf{r} = (x, y)$ incorporates one fermion $c_{\mathbf{r}}^\dagger$. At each time step, unitary gates and measurements are applied to bonds of a specific color, following the sequence shown at the bottom of Fig. S1 (a). The unitary gate on the bond connecting sites \mathbf{r} and \mathbf{r}' is $U = \exp[i\theta t_{\mathbf{r}\mathbf{r}'}(c_{\mathbf{r}}^\dagger c_{\mathbf{r}'} + c_{\mathbf{r}'}^\dagger c_{\mathbf{r}})]$. The hopping coefficient $t_{\mathbf{r}\mathbf{r}'}$ follows the Harper-Hofstadter Hamiltonian [17] with a flux of $1/2$ quantum per plaquette: $t_{\mathbf{r}, \mathbf{r}+e_x} = t$, $t_{\mathbf{r}, \mathbf{r}+e_y} = t(-1)^x$. Weak measurements are performed on the

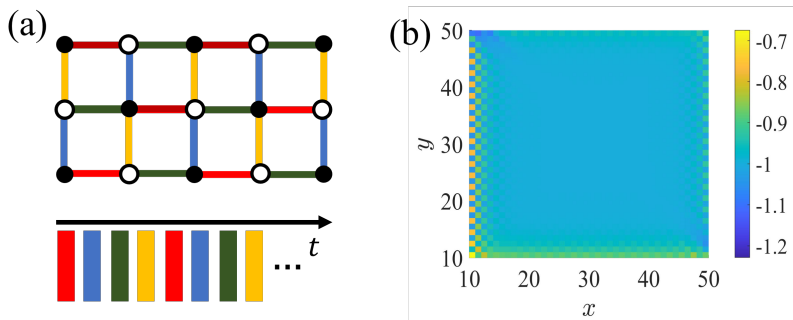


FIG. S1. (a) $(2+1)$ -dimensional quantum circuit on a lattice of size $L_x \times L_y$. Each site \mathbf{r} incorporates one fermion $c_{\mathbf{r}}^\dagger$. At each time step, measurements and unitary gates are applied to the bonds of a specific color, following the sequence shown at the bottom. (b) Local Chern marker of the steady state with the homogeneous measurement strength.

occupations of the bonding state $d^\dagger d$ and antibonding state $f^\dagger f$ with $d = 1/\sqrt{2}(c_{\mathbf{r}} + c_{\mathbf{r}'})$ and $f = 1/\sqrt{2}(c_{\mathbf{r}} - c_{\mathbf{r}'})$. The corresponding Kraus operators are $K_{d\pm} = (2 \cosh \Gamma)^{-1} e^{\pm \Gamma (d^\dagger d - 1/2)}$ and $K_{f\pm} = (2 \cosh \Gamma)^{-1} e^{\pm \Gamma (f^\dagger f - 1/2)}$, respectively. We postselect measurement outcomes as follows. If the hopping on the bond is $t_{\mathbf{r}\mathbf{r}'} = t$, we select K_{d+} and K_{f-} ; if the hopping on the bond is $t_{\mathbf{r}\mathbf{r}'} = -t$, we select K_{d-} and K_{f+} .

We begin with a scenario where the measurement strengths are uniform across all bonds and constant over time, preserving translation invariance both temporally and spatially. Let K_i ($i = 1, 2, 3, 4$) represent the nonunitary time evolution operator that describes the combined effect of the unitary operator and the postselected Kraus operator acting on the bonds of the i th color in Fig. S1 (a). The nonunitary time evolution after N cycles of operations is given by K^N , with $K = K_4 K_3 K_2 K_1$. Let $\lambda_1, \lambda_2, \dots, \lambda_N$ be the eigenvalues of K ($N = L^2$ with L being the system size). We sort λ_i 's such that $|\lambda_1| \geq |\lambda_2| \geq \dots \geq |\lambda_p| > 1 > |\lambda_{p+1}| \geq \dots \geq |\lambda_N|$. For this model, we find that the number of eigenvalues satisfying $|\lambda_i| > 1$ is $p = L^2/2$ and we have $|\lambda_i| \neq 1$ for all i . The Lyapunov exponents η_i 's of K^N are given by $\eta_i = \ln |\lambda_i|$. The steady state is $|\Psi_S\rangle \propto \prod_{n=1}^p \left(\sum_i c_i^\dagger (S_R)_{ni} \right) |0\rangle$, where $(S_R)_n$ is the n th right eigenvector of K with eigenvalues $|\lambda_n| > 1$ ($n = 1, 2, \dots, p$), and $|0\rangle$ is the empty state.

In the numerical simulation, we choose the parameters as $t = 1$, $\theta = \pi/3$, and $\Gamma = 1$. To evaluate the local Chern marker of the steady state, we calculate its correlation function. We perform the QR decomposition on S_R : $S_R = UR$, where U is an $N \times p$ matrix U satisfying $U^\dagger U = 1_{p \times p}$, and R is an upper triangular matrix. The correlation matrix $D_{ij} = \langle \Psi_S | c_i^\dagger c_j | \Psi_S \rangle$ of the steady state is given by $D = U^* U^T$. The local Chern marker $C(\mathbf{r})$ is [16, 18]

$$C(\mathbf{r}) = \frac{1}{2\pi i} (DXDYD - DYDXD)_{\mathbf{r},\mathbf{r}} \quad (\text{S20})$$

with the position operator $X_{\mathbf{r},\mathbf{r}'} = \delta_{\mathbf{r},\mathbf{r}'} x$ and $Y_{\mathbf{r},\mathbf{r}'} = \delta_{\mathbf{r},\mathbf{r}'} y$. As shown in Fig. S1 (b), the local Chern marker is quantized to be $C(\mathbf{r}) \approx -1$ in the central region of the lattice.

Next, we consider a scenario where measurement strengths vary randomly among bonds and time. We suppose that the measurement strength for each bond at each time is distributed uniformly and independently in the range of $[\Gamma - W/2, \Gamma + W/2]$. We here choose the parameter as $W = 0.4$, and the other parameters to be the same as in the previous case. Moreover, the system size is $L_x \times L_y = 40 \times 40$, and the evolution time is set to 10^4 cycles. To simulate this time-dependent nonunitary evolution and evaluate its Lyapunov exponents, we employ an algorithm based on the QR decomposition, similar to the one discussed in Sec. IV B. Additional details can also be found in Refs. [9, 19].

-
- [S1] K. Kawabata, K. Shiozaki, M. Ueda, and M. Sato, Symmetry and Topology in Non-Hermitian Physics, *Phys. Rev. X* **9**, 041015 (2019).
[S2] M. R. Zirnbauer, Riemannian symmetric superspaces and their origin in random-matrix theory, *J. Math. Phys.* **37**, 4986 (1996).
[S3] F. Evers and A. D. Mirlin, Anderson transitions, *Rev. Mod. Phys.* **80**, 1355 (2008).
[S4] M. Karoubi, *K-Theory: An Introduction* (Springer, Berlin, Heidelberg, 1978).
[S5] S. Ryu, A. P. Schnyder, A. Furusaki, and A. W. W. Ludwig, Topological insulators and superconductors: tenfold way and dimensional hierarchy, *New J. Phys.* **12**, 065010 (2010).
[S6] Z. Gong, Y. Ashida, K. Kawabata, K. Takasan, S. Higashikawa, and M. Ueda, Topological Phases of Non-Hermitian Systems, *Phys. Rev. X* **8**, 031079 (2018).

- [S7] K. Jacobs and D. A. Steck, A straightforward introduction to continuous quantum measurement, *Contemp. Phys.* **47**, 279 (2006).
- [S8] H. M. Wiseman and G. J. Milburn, *Quantum Measurement and Control* (Cambridge University Press, Cambridge, England, 2009).
- [S9] Z. Xiao, T. Ohtsuki, and K. Kawabata, Universal Stochastic Equations of Monitored Quantum Dynamics (2024), arXiv:2408.16974.
- [S10] F. J. Dyson, The Dynamics of a Disordered Linear Chain, *Phys. Rev.* **92**, 1331 (1953).
- [S11] P. W. Brouwer, C. Mudry, B. D. Simons, and A. Altland, Delocalization in Coupled One-Dimensional Chains, *Phys. Rev. Lett.* **81**, 862 (1998).
- [S12] I. Mondragon-Shem, T. L. Hughes, J. Song, and E. Prodan, Topological Criticality in the Chiral-Symmetric AIII Class at Strong Disorder, *Phys. Rev. Lett.* **113**, 046802 (2014).
- [S13] A. Altland, D. Bagrets, L. Fritz, A. Kamenev, and H. Schmiedt, Quantum Criticality of Quasi-One-Dimensional Topological Anderson Insulators, *Phys. Rev. Lett.* **112**, 206602 (2014).
- [S14] N. Hatano and D. R. Nelson, Localization Transitions in Non-Hermitian Quantum Mechanics, *Phys. Rev. Lett.* **77**, 570 (1996).
- [S15] N. Hatano and D. R. Nelson, Vortex pinning and non-Hermitian quantum mechanics, *Phys. Rev. B* **56**, 8651 (1997).
- [S16] J. D. Hannukainen, M. F. Martínez, J. H. Bardarson, and T. K. Kivring, Local Topological Markers in Odd Spatial Dimensions and Their Application to Amorphous Topological Matter, *Phys. Rev. Lett.* **129**, 277601 (2022).
- [S17] P. G. Harper, Single Band Motion of Conduction Electrons in a Uniform Magnetic Field, *Proc. Phys. Soc. A* **68**, 874 (1955).
- [S18] E. Prodan, T. L. Hughes, and B. A. Bernevig, Entanglement Spectrum of a Disordered Topological Chern Insulator, *Phys. Rev. Lett.* **105**, 115501 (2010).
- [S19] X. Cao, A. Tilloy, and A. De Luca, Entanglement in a fermion chain under continuous monitoring, *SciPost Phys.* **7**, 024 (2019).